Published in final edited form as:
Eur J Radiol. 2014 December ; 83(12): 2109–2113. doi:10.1016/j.ejrad.2014.09.003.

Intravoxel Incoherent Motion Diffusion Imaging of the Liver: Optimal b-value Subsampling and Impact on Parameter Precision and Reproducibility

Hadrien Dyvorne, PhD[1], **Guido Jajamovich, PhD**[1], **Suguru Kakite, MD**[1], **Bernd Kuehn, PhD**[2], and **Bachir Taouli, MD**[1]

Hadrien Dyvorne: hadrien.dyvorne@mountsinai.org; Guido Jajamovich: guido.jajamovich@mountsinai.org; Suguru Kakite: sugkaki@med.tottori-u.ac.jp; Bernd Kuehn: bernd.kuehn@siemens.com; Bachir Taouli: bachir.taouli@mountsinai.org

[1]Department of Radiology, Translational and Molecular Imaging Institute, Mount Sinai School of Medicine, One Gustave Levy Place, New York, NY 10029 USA

[2]Siemens AG, Healthcare Sector, Erlangen, Germany

Abstract

Purpose—To increase diffusion sampling efficiency in intravoxel incoherent motion (IVIM) diffusion-weighted imaging (DWI) of the liver by reducing the number of diffusion weightings (b-values).

Materials and Methods—In this IRB approved HIPAA compliant prospective study, 53 subjects (M/F 38/15, mean age 52 ± 13 y) underwent IVIM DWI at 1.5 T using 16 b-values (0 to 800 s/mm^2), with 14 subjects having repeat exams to assess IVIM parameter reproducibility. A biexponential diffusion model was used to quantify IVIM hepatic parameters (PF: perfusion fraction, D: true diffusion and D*: pseudo diffusion). All possible subsets of the 16 b-values were probed, with number of b values ranging from 4 to 15, and corresponding parameters were quantified for each subset. For each b-value subset, global parameter estimation error was computed against the parameters obtained with all 16 b-values and the subsets providing the lowest error were selected. Interscan estimation error was also evaluated between repeat exams to

Corresponding author: Bachir Taouli, Mount Sinai School of Medicine, Body MRI and Translational and Molecular Imaging Institute, One Gustave Levy Place, Box 1234, New York, NY 10029 USA, bachir.taouli@mountsinai.org, Tel: (212) 241-2642, Fax: (212) 427-8137.

Hadrien Dyvorne, PhD, Icahn School of Medicine at Mount Sinai
Guido Jajamovich, PhD, Icahn School of Medicine at Mount Sinai
Suguru Kakite, MD, Division of Radiology, Tottori University
Bernd Kuehn, PhD, Siemens AG, Healthcare Sector, Erlangen, Germany
Bachir Taouli, MD, Icahn School of Medicine at Mount Sinai

***Conflict of Interest**

Hadrien Dyvorne, Guido Jajamovich, Suguru Kakite have no conflict of interest to declare.

Bachir Taouli has no conflict of interest to declare related to this work. Not related to this work: B.T. is consultant for Bayer Healthcare.

Bernd Kuehn has no conflict of interest to declare related to this work. Not related to this work: B.K. is an employee of Siemens Healthcare.

assess reproducibility of the IVIM technique in the liver. The optimal b-values distribution was selected such that the number of b-values was minimal while keeping parameter estimation error below interscan reproducibility error.

Results—As the number of b-values decreased, the estimation error increased for all parameters, reflecting decreased precision of IVIM metrics. Using an optimal set of 4 b-values (0, 15, 150 and 800 s/mm^2), the errors were 6.5, 22.8 and 66.1 % for D, PF and D* respectively. These values lie within the range of test-retest reproducibility for the corresponding parameters, with errors of 12.0, 32.3 and 193.8 % for D, PF and D* respectively.

Conclusion—A set of 4 optimized b-values can be used to estimate IVIM parameters in the liver with significantly shorter acquisition time (up to 75 %), without substantial degradation of IVIM parameter precision and reproducibility compared to the 16 b-value acquisition used as the reference.

Keywords

Diffusion weighted imaging; b-value; perfusion; pseudo-diffusion; optimization; liver; intravoxel incoherent motion

INTRODUCTION

Diffusion weighted imaging (DWI) has been extensively investigated in abdominal organs such as the liver, kidneys and pancreas, using molecular diffusion as a marker of tissue structure in healthy and pathologic tissue (1–10). Additionally, extracting tissue perfusion using intravoxel incoherent motion (IVIM) DWI has the potential to detect and characterize focal liver lesions and diffuse parenchymal disease (3, 11–16). In spite of an increasing number of applications of DWI without or with IVIM, there is no clear consensus regarding the optimal protocol to be used. One crucial question pertains to the diffusion-encoding strategy, which defines the ability to separate blood perfusion from true diffusion effects via a proper choice of the number and distribution of diffusion weightings, or b-values. Previous abdominal IVIM DWI studies have used ad hoc distributions of 5 to 16 b-values that sample both perfusion (≤ 100 s/mm^2) and diffusion (> 100 s/mm^2) regimes (12–15). Because more b-value samples involve longer scan time, there is a need to use the smallest possible number of b-values. We hypothesize that the number of b-values could be reduced while still enabling correct IVIM parameter estimation, without affecting the reproducibility of the technique.

Two recent studies have proposed methods for optimizing b-value sampling for IVIM. Zhang et al (17) used an error propagation model to determine the best set of b-values in the renal parenchyma and renal lesions. Lemke et al (18) have proposed a series of b-values by sequentially adding b-values that minimize the fit errors for a range of IVIM parameters in the pancreas. Both studies used IVIM model decay curves with added Gaussian noise, with optimal b-values distributions chosen such that the errors in estimated D, PF and D* were minimized. Although these model-based approaches yield interesting results, they have limitations. First, the models assume a Gaussian noise figure. Physiologic signal fluctuations in a diffusion experiment could result in more complex noise properties that may be difficult

to model. Another restriction is the consideration of fixed IVIM parameters in simulations, while a population with liver disease may present a wide range of parameters, thus making the proposed optimal b-value distributions less robust.

The purpose of this study is to present a data-driven descriptive analysis of liver IVIM parameter precision when a small set of b-values is used for parameter computation, and to determine the minimal number and optimal distribution of b-values necessary for reproducible IVIM parameter quantification in the liver.

MATERIALS AND METHODS

Subjects

This HIPAA compliant prospective study funded by NIDDK was approved by the local institution review board, and included a total of 53 subjects (M/F 38/15, mean age 52 ± 13 y) enrolled in a prospective liver fibrosis study at 1.5T with written consent obtained prior to the exam. The data from 20 of these 53 subjects has been used in a previous study that assessed the test-retest reproducibility of IVIM measurement (19). Seven subjects were healthy volunteers and 46 subjects had liver disease (43 with chronic hepatitis C infection, 3 with nonalcoholic steatohepatitis).

MRI acquisition

MRI exams were performed at 1.5T (Magnetom Avanto, Siemens Healthcare). The IVIM DWI sequence (Table 1) sampled 16 b-values using bipolar diffusion gradients (20), and 3 diffusion directions per b-value, combined to yield an estimate of the diffusion trace. 15 interleaved slices were acquired in coronal orientation (chosen to match the orientation of dynamic contrast enhanced series acquired in the same exam). The effects of respiratory motion were reduced using a navigator echo gating at end expiration. In addition to being widely available and routinely used, this acquisition method was shown in a previous study to yield better reproducibility for liver IVIM than a free breathing acquisition, and to reduce eddy current artifacts compared to a Stejskal-Tanner method (19, 20). The distribution of b-values was chosen to describe faster pseudo diffusion regime (b <200 s/mm^2) in steps of 15 s/mm^2 and slower molecular diffusion regime (b >200 s/mm^2) in steps of 200 s/mm^2. The average acquisition time was 10:54 ± 4:38 min (ranging from 6:10 to 23:34 min), and varied according to the subject's breathing.

Image analysis

Regions of interest (ROIs, mean area 5 cm^2 per ROI) were drawn on the diffusion-weighted images by an experienced observer (–, with 3 year experience in image processing) using Osirix Dicom viewer, in the right hepatic lobe on 3 adjacent slices centered at the level of the portal vein bifurcation (Fig. 1). The left lobe was not included in the analysis due to the presence of cardiac motion artifacts affecting high b-value images. Mean ROI signal intensity of the diffusion-weighted signal was used to derive true diffusion D, pseudo diffusion D* and perfusion fraction PF defining the signal decay in the IVIM equation:

$$SI_N(b) = PFe^{-bD*} + (1 - PF)e^{-bD} \quad (1)$$

Where $SI_N(b)$ is the signal intensity at for a given b-value, normalized to the signal intensity value at b=0 s/mm^2, and b is the b-value reflecting the effects of diffusion-weighting gradients. Although different models have been proposed for perfusion-related decay in a DWI experiment (21), we selected the pseudo-diffusion model because of its extensive use in the abdominal applications and its relative simplicity. IVIM parameters were estimated using a nonlinear least square fit to the biexponential model curve (15, 22) implemented locally using Matlab (R2012b). For the fit routine, initial parameters were derived from the high b-value decay for D (b >120 s/mm^2), the intercept at b = 0 s/mm^2 for PF and the low b-values decay for D* (b <120 s/mm^2). Parameters were constrained within the following boundaries: D (10^{-5} – 10^{-2} mm^2/s), PF (0 – 60 %) and D* (10^{-3}–5.10^{-1} mm^2/s).

In addition to IVIM decay curves, we measured the estimated signal to noise ratio (eSNR) as the mean ROI signal intensity divided by the standard deviation of the signal intensity of an ROI placed in the background.

Optimization of b-values and estimation of precision of IVIM parameters

Lemke et al (18) observed that, provided sufficient SNR, an ad hoc 16 b-value distribution from the literature (13) provides performance similar to optimized distributions for IVIM parameter estimation. However, using an ad hoc distribution with a large number of b-values will increase the scan time. For clinical applications, there is a need to achieve the shortest possible scan time, which can be obtained by decreasing the number of b-values by carefully selecting an optimal small set of b-values.

Our approach to finding the optimal number and distribution of b-values consisted in electing sub-distributions that minimize the global parameter error (18) defined by $\sigma_{sub} = \sigma_D + \sigma_{PF} + \sigma_{D*}$, where for each IVIM parameter P:

$$\sigma_P = \sqrt{\left\langle \left(\frac{P_{sub} - P_{ref}}{P_{ref}} \right)^2 \right\rangle} \quad (3)$$

P_{ref} is an IVIM parameter derived using the 16 b-value distribution, considered as reference parameters, and P_{sub} is derived using a subset of the 16 b-value distribution. The brackets represent averaging over the whole population (n=53 subject).

For every allowed number of b-values from 4 to 15, we selected the optimal distribution of b-values such that the global error σ would be minimized. A brute force approach (an algorithm that explores all possible combinations of subsets of 16 b-values) was adopted. Although computationally intensive (64,838 subsets were computed), this approach is guaranteed to find the global minimum among all possible subsets. As the parameter deviation is expected to increase with decreasing number of b-values, we defined the optimal number of b-values such that the minimum global error σ_{sub} for that number of b-values would be lower than reference parameter reproducibility (computed with all 16 b-values, see below).

Reproducibility of the IVIM technique

Among the population, 14 subjects (M/F 10/4, mean age 41 ± 15 y) underwent two exams (mean delay 16 days, range 5 – 44 days) to assess test-retest reproducibility of IVIM DWI. The reproducibility was expressed using the interscan error $\sigma_{repeat} = \sigma_D + \sigma_{PF} + \sigma_{D*}$, where for each IVIM parameter P:

$$\sigma_P = \sqrt{\langle \left(\frac{P_{scan2} - P_{scan1}}{P_{scan1}} \right)^2 \rangle} \quad (4)$$

Where P_{scan2} and P_{scan1} are the IVIM parameters of test and retest scans, derived using 16 b-values, and the brackets represent averaging over the all subjects who underwent repeat exams (n=14).

RESULTS

Reference parameters computed using 16 b-values and reproducibility of the technique

Parameter values obtained with 16 b-values (used as the reference) and ranges are given in Table 2. Parameter convergence during the nonlinear least squares fitting was within parameter limits in all cases except in 5 subjects, where the upper limit was reached for D*. The average eSNR at b = 800 s/mm^2 was 51.6 ± 20.6. The test-retest reproducibility of parameter estimation (Table 2) was highest for D, intermediate for PF and lowest for D* with σ_{repeat} of 12.0 %, 32.3 % and 193.8 % respectively.

Parameter evolution when decreasing the number of b-values

Table 3 lists all joint optimal distributions from 15 to 4 b-values and Fig. 1 shows the evolution of Bland-Altman SD subset for the optimum subset as a function of the number of b-values. As the number of b-values decreased, there was an increase in deviations from the reference parameters. A similar trend was followed by all parameters, although larger deviations were observed for D* (up to 66.1%), followed by PF (up to 22.8 %) and D (up to 6.5 %). Fig. 2 shows an example of parametric maps derived using optimal distributions of 4, 8 and 12 b-values given in Table 3. Similar maps were observed in the liver parenchyma.

Choice of optimal b-value distribution

The aim of the optimization is to select a minimal number of optimally sampled b-values, such that parameter precision degradation lies within the test-retest reproducibility of the technique at 16 b-values. Fig. 1 shows parameter interscan error σ_{repeat} for 16 b-values, along with parameter subset error σ_{subset}. For any distribution size, σ_{subset} is lower than σ_{repeat}, therefore a 4 b-values distribution (0, 15, 150, 800 s/mm^2) reaches the b-value optimization criteria.

DISCUSSION

By evaluating both blood perfusion and molecular diffusion components in tissues, IVIM DWI has the potential to help characterize diffuse liver disease (13, 15), focal liver and pancreatic lesions (14, 23, 24) and renal function (25, 26). However, the separation of

diffusion and pseudo diffusion requires multiple b-values that, if coupled with signal averaging, multiple diffusion direction measurements and/or navigator gated acquisition, may result in prohibitively long scan times. We have optimized b-value sampling for IVIM DWI based on in vivo data acquired in the liver on 53 subjects. To achieve this, we have subsampled datasets from an initial 16 b-values distribution and selected the optimal distributions that achieved the lowest estimated parameter deviation for different number of b-values ranging from 4 to 15. As the number of b-values decreased, we observed higher deviation from the reference parameters. The effect of b-value subsampling on test-retest IVIM parameter reproducibility was found to be negligible even when using an optimal 4 b-values distribution which deviated minimally from the reference distribution using 16 b-values.

Previous IVIM studies in the liver have used 5 to 10 b-values (12, 13, 15) with different distributions. In order to optimize the choice of b-values, two model-based approaches have already been investigated. Zhang et al (17) proposed distributions of 4 to 10 b-values for the kidney, while Lemke et al (18) proposed sequences of 3 to 35 b-values, the nature and the length of which can be selected depending on the perfusion regime, the desired precision and the available SNR. However, model-based optimization strategies rely on assumptions, such as signal to noise behavior, which may be invalidated for in vivo data in the presence of artifacts arising from subject motion, magnetic susceptibility and gradients eddy currents. Our strategy offers a data-driven optimization for IVIM acquisition in the liver.

The quality of IVIM data depends on the available SNR as well as the presence of artifacts that may affect the reproducibility of IVIM parameter estimation. Factors such as the platform (manufacturer, field strength) or the type of acquisition (diffusion gradients, motion compensation) may influence data quality, resulting in variable performance. In order to reduce artifacts, we used intrinsic eddy current attenuation with bipolar diffusion gradients and respiratory motion control using navigator tracking (19). Parameter reproducibility was good for D ($\sigma_{repeat} < 20$ %), intermediate for PF ($\sigma_{repeat} < 40$ %) and poor for D* ($\sigma_{repeat} > 40$ %). These findings are similar to previous work assessing inter-scan reproducibility of the IVIM technique: Patel et al (15) reported coefficients of variation of 5.0% (D), 11.4% (PF) and 23.8% (D*) in 5 subjects using 9 b-values, and Andreou et al (27) reported confidence intervals of −5.12–9.09 (D), −24.3–25.1 (PF) and −31.2–59.1 (D*) in 14 subjects using 8 b-values. D* reproducibility was significantly worse in our study, which may be due to a wider parameter range allowed by our fitting method. Furthermore, we anticipate that the reproducibility evaluated in a prospective 4 b-value acquisition should be similar or better, because a shorter acquisition time might result in reduced motion artifacts. This would have to be evaluated in a future study.

To select the minimum number of b-values required for precise IVIM parameter estimation, one has to balance the loss in parameter estimation quality with a reduction in acquisition time. In practice, an optimized distribution with 4 b-values yields parameter deviations within the test-retest reproducibility of a 16 b-value acquisition, while reducing scan time by up to 75% compared to 16 b-values.

There are limitations to this study. Because we retrospectively subsampled existing data, the b-values and signal averaging per b-value were fixed, thus restricting the search for an optimum to available b-values only. However, the 16 b-value distribution given in Table 1 presents dense sampling both the pseudo-diffusion and true diffusion regime, and could thus undergo subsampling to be further optimized. Furthermore, minimal improvement if the 16 b-values parameter computation would be expected with increased averaging, given the relatively high signal to noise ratio of our dataset (>50). Finally, this study only addressed optimization when considering the liver. Further work is needed in different organs as well as for focal lesions using IVIM.

In conclusion, it is possible to reduce the number of required b-values in IVIM applications for the liver, while preserving a good performance for parameter estimation. Using an optimized 4 b-values distribution (0, 15, 150 and 800 s/mm^2), the scan time can be significantly reduced by up to 75% compared to a 16 b-values ad hoc distribution, without affecting IVIM diffusion parameter precision and test-retest reproducibility.

Acknowledgments

This research was funded by NIDDK Grant 1R01DK087877.

Abbreviations

eSNR	estimated signal to noise ratio
D	molecular diffusion coefficient
D*	pseudo diffusion coefficient
DWI	diffusion-weighted imaging
IVIM	intravoxel incoherent motion
PF	perfusion fraction
ROI	region of interest

References

1. Taouli B, Vilgrain V, Dumont E, Daire JL, Fan B, Menu Y. Evaluation of liver diffusion isotropy and characterization of focal hepatic lesions with two single-shot echo-planar MR imaging sequences: prospective study in 66 patients. Radiology. 2003; 226(1):71–8. [PubMed: 12511671]
2. Thoeny HC, De Keyzer F, Oyen RH, Peeters RR. Diffusion-weighted MR imaging of kidneys in healthy volunteers and patients with parenchymal diseases: initial experience. Radiology. 2005; 235(3):911–7. [PubMed: 15845792]
3. Koh DM, Scurr E, Collins DJ, et al. Colorectal hepatic metastases: quantitative measurements using single-shot echo-planar diffusion-weighted MR imaging. Eur Radiol. 2006; 16(9):1898–905. [PubMed: 16691378]
4. Muhi A, Ichikawa T, Motosugi U, et al. High-b-value diffusion-weighted MR imaging of hepatocellular lesions: estimation of grade of malignancy of hepatocellular carcinoma. J Magn Reson Imaging. 2009; 30(5):1005–11. [PubMed: 19856432]
5. Akisik MF, Aisen AM, Sandrasegaran K, et al. Assessment of chronic pancreatitis: utility of diffusion-weighted MR imaging with secretin enhancement. Radiology. 2009; 250(1):103–9. [PubMed: 19001148]

6. Taouli B, Koh DM. Diffusion-weighted MR imaging of the liver. Radiology. 2010; 254(1):47–66. [PubMed: 20032142]
7. Rosenkrantz AB, Niver BE, Fitzgerald EF, Babb JS, Chandarana H, Melamed J. Utility of the apparent diffusion coefficient for distinguishing clear cell renal cell carcinoma of low and high nuclear grade. AJR Am J Roentgenol. 2010; 195(5):W344–51. [PubMed: 20966299]
8. Wang Y, Miller FH, Chen ZE, et al. Diffusion-weighted MR imaging of solid and cystic lesions of the pancreas. Radiographics. 2011; 31(3):E13–30. [PubMed: 21415179]
9. Sandrasegaran K, Sundaram CP, Ramaswamy R, et al. Usefulness of diffusion-weighted imaging in the evaluation of renal masses. AJR Am J Roentgenol. 2010; 194(2):438–45. [PubMed: 20093607]
10. Park MS, Kim S, Patel J, et al. Hepatocellular carcinoma: detection with diffusion-weighted versus contrast-enhanced magnetic resonance imaging in pretransplant patients. Hepatology. 2012; 56(1): 140–8. [PubMed: 22370974]
11. Mulkern RV, Barnes AS, Haker SJ, et al. Biexponential characterization of prostate tissue water diffusion decay curves over an extended b-factor range. Magn Reson Imaging. 2006; 24(5):563–8. [PubMed: 16735177]
12. Yamada I, Aung W, Himeno Y, Nakagawa T, Shibuya H. Diffusion coefficients in abdominal organs and hepatic lesions: evaluation with intravoxel incoherent motion echo-planar MR imaging. Radiology. 1999; 210(3):617–23. [PubMed: 10207458]
13. Luciani A, Vignaud A, Cavet M, et al. Liver cirrhosis: intravoxel incoherent motion MR imaging–pilot study. Radiology. 2008; 249(3):891–9. [PubMed: 19011186]
14. Lemke A, Laun FB, Klauss M, et al. Differentiation of pancreas carcinoma from healthy pancreatic tissue using multiple b-values: comparison of apparent diffusion coefficient and intravoxel incoherent motion derived parameters. Invest Radiol. 2009; 44(12):769–75. [PubMed: 19838121]
15. Patel J, Sigmund EE, Rusinek H, Oei M, Babb JS, Taouli B. Diagnosis of cirrhosis with intravoxel incoherent motion diffusion MRI and dynamic contrast-enhanced MRI alone and in combination: preliminary experience. J Magn Reson Imaging. 2010; 31(3):589–600. [PubMed: 20187201]
16. Sigmund EE, Vivier PH, Sui D, et al. Intravoxel incoherent motion and diffusion-tensor imaging in renal tissue under hydration and furosemide flow challenges. Radiology. 2012; 263(3):758–69. [PubMed: 22523327]
17. Zhang JL, Sigmund EE, Rusinek H, et al. Optimization of b-value sampling for diffusion-weighted imaging of the kidney. Magn Reson Med. 2012; 67(1):89–97. [PubMed: 21702062]
18. Lemke A, Stieltjes B, Schad LR, Laun FB. Toward an optimal distribution of b values for intravoxel incoherent motion imaging. Magn Reson Imaging. 2011; 29(6):766–76. [PubMed: 21549538]
19. Dyvorne HA, Galea N, Nevers T, et al. Diffusion-weighted imaging of the liver with multiple b values: effect of diffusion gradient polarity and breathing acquisition on image quality and intravoxel incoherent motion parameters–a pilot study. Radiology. 2013; 266(3):920–9. [PubMed: 23220895]
20. Reese TG, Heid O, Weisskoff RM, Wedeen VJ. Reduction of eddy-current-induced distortion in diffusion MRI using a twice-refocused spin echo. Magn Reson Med. 2003; 49(1):177–82. [PubMed: 12509835]
21. Henkelman RM, Neil JJ, Xiang QS. A quantitative interpretation of IVIM measurements of vascular perfusion in the rat brain. Magn Reson Med. 1994; 32(4):464–9. [PubMed: 7997111]
22. Cho GY, Kim S, Jensen JH, Storey P, Sodickson DK, Sigmund EE. A versatile flow phantom for intravoxel incoherent motion MRI. Magn Reson Med. 2012; 67(6):1710–20. [PubMed: 22114007]
23. Kang KM, Lee JM, Yoon JH, Kiefer B, Han JK, Choi BI. Intravoxel Incoherent Motion Diffusion-weighted MR Imaging for Characterization of Focal Pancreatic Lesions. Radiology. 2013
24. Yoon JH, Lee JM, Yu MH, Kiefer B, Han JK, Choi BI. Evaluation of hepatic focal lesions using diffusion-weighted MR imaging: Comparison of apparent diffusion coefficient and intravoxel incoherent motion-derived parameters. J Magn Reson Imaging. 2013
25. Thoeny HC, Zumstein D, Simon-Zoula S, et al. Functional evaluation of transplanted kidneys with diffusion-weighted and BOLD MR imaging: initial experience. Radiology. 2006; 241(3):812–21. [PubMed: 17114628]

26. Eckerbom P, Hansell P, Bjerner T, Palm F, Weis J, Liss P. Intravoxel incoherent motion MR imaging of the kidney: pilot study. Adv Exp Med Biol. 2013; 765:55–8. [PubMed: 22879014]

27. Andreou A, Koh DM, Collins DJ, et al. Measurement reproducibility of perfusion fraction and pseudodiffusion coefficient derived by intravoxel incoherent motion diffusion-weighted MR imaging in normal liver and metastases. Eur Radiol. 2012

- We present an optimization method for liver IVIM (intravoxel incoherent motion) DWI (diffusion-weighted imaging), to reduce the number of sampled b-values.
- Using experimental liver DWI datasets with 16 b-values acquired in 53 subjects, we assessed the precision of parameter quantification using combinatorial subsets of 4 to 15 b-values using the 16 b-values combination used as the reference.
- In addition, we analyzed the effect of b-value subsampling on interscan reproducibility of IVIM measurements.
- We found that liver IVIM can be performed using an optimal distribution of 4 b values (0, 15, 150, 800 s/mm^2) without affecting parameter precision and reproducibility.

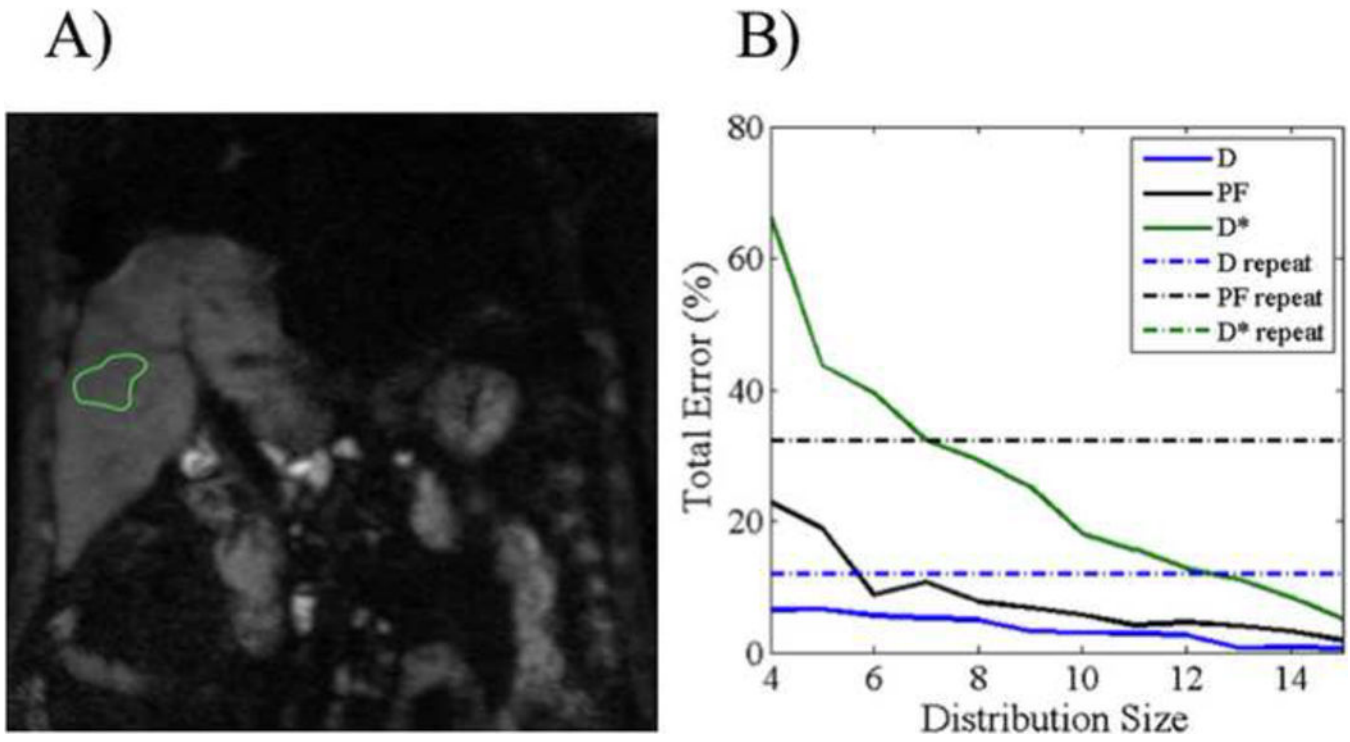

Fig. 1.

Left: example of region of interest placement in the liver in coronal acquisition (b=800 s/mm^2). The average signal intensity was used to extract IVIM diffusion parameters using biexponential fitting. Right: Evolution of the error for each IVIM parameters (D in blue, D* in green, and PF in black) of optimal b-values subsets (as given in Table 3) compared to 16 b-values reference parameters. The dashed lines indicate the 16 b-values test-retest error for each parameter (D* reproducibility lies outside the graph, as shown by the arrow). For any number of b-values down to 4, deviations of IVIM parameters from the 16 b-values distribution were within the test-retest error.

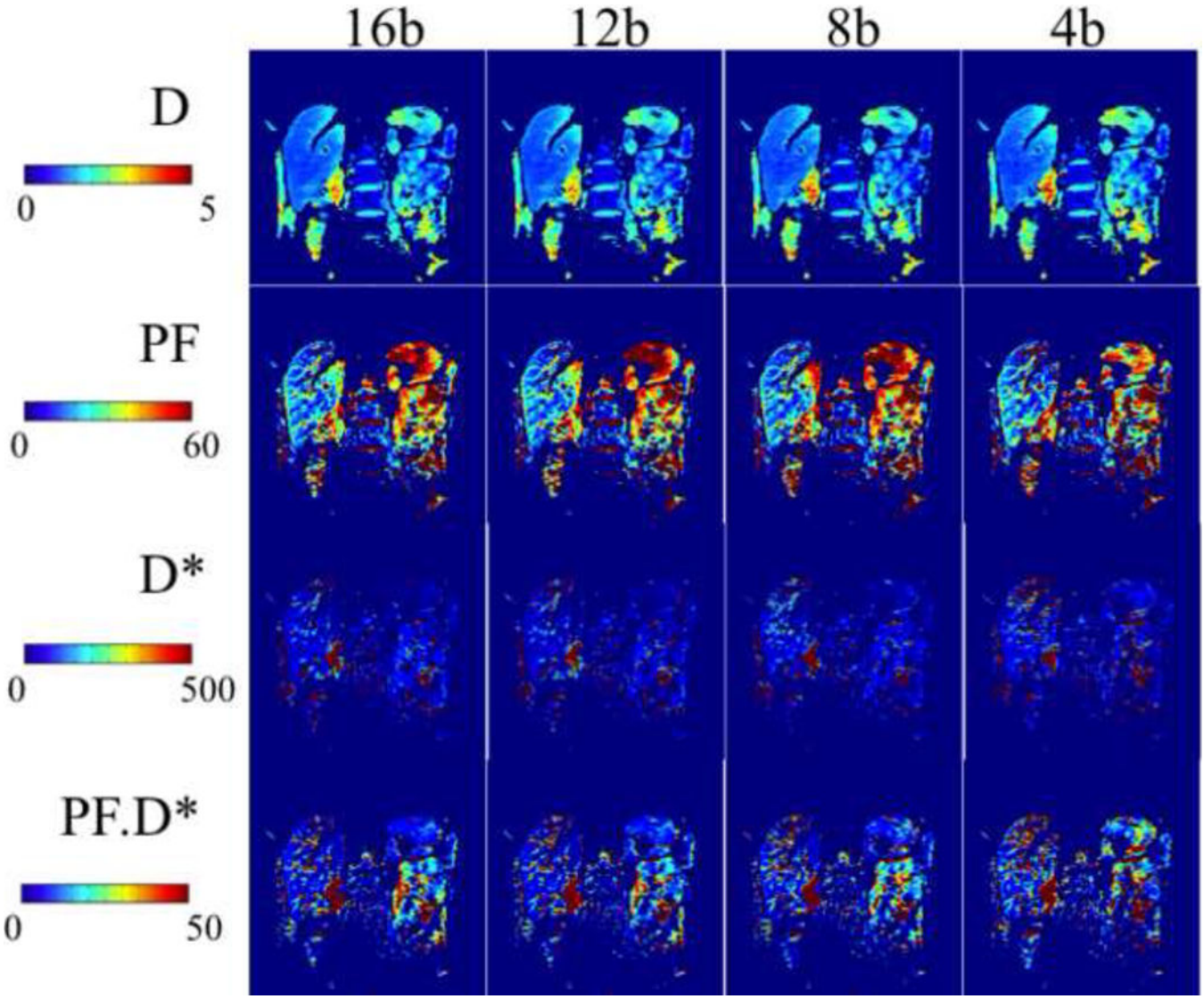

Fig. 2.

Example of IVIM parametric maps in a 64 year-old male patient with chronic hepatitis C. Parameters were derived using 16, 12, 8 and 4 b-values with distributions given in Table 3. Similar parametric maps were observed in the liver. Parameter values from ROI analysis were D = 1.12, 1.13, 1.12 and 1.08 10^{-3} mm^2/s, PF = 11.8, 12.4, 12.0 and 14.0 %, and D* = 87.5, 78.1, 106.3 and 78.1 10^{-3} mm^2/s for the 16, 12, 8 and 4 b-value acquisitions respectively.

Table 1

Imaging parameters for IVIM DWI acquisitions of the abdomen at 1.5T.

b-values (s/mm^2)	0, 15, 30, 45, 60, 75, 90, 105, 120, 135, 150, 175, 200, 400, 600, 800
Respiration control	Navigator triggered
TR	One respiratory cycle
TE (ms)	74
FOV	370 × 370
Matrix size	160 × 128
Orientation	Coronal
Slice thickness/interval (mm)	8/1.6
Signal averaging	2
Parallel imaging	GRAPPA R=2
Acquisition time (min)	10:54 ± 4:38 (6:10–23:34)

Table 2

Liver IVIM DWI parameters values and reproducibility using a combination of 16 b-values expressed in terms of the normalized Bland Altman standard deviation in 53 subjects.

	D	PF	D*
Parameter value*	1.11 ± 0.16	12.9 ± 4.9	136 ± 130
Parameter range	0.85–1.70	3.3–24.9	26.1–500.0
Reproducibility error (%)	12.0	32.3	193.8

* expressed as mean ± standard deviation of population parameter values.

D: true diffusion (10^3 mm^2/s), D*: pseudo-diffusion (10^3 mm^2/s), PF: perfusion fraction (%)

Table 3

Optimal b-value distributions that minimize liver IVIM parameter deviations with respect to a 16 b-values distribution.

4b	5b	6b	7b	8b	9b	10b	11b	12b	13b	14b	15b
0	0	0	0	0	0	0	0	0	0	0	0
15	15	15	15	15	15	15	15	15	15	15	15
150	90	90	60	60	30	30	30	30	30	30	30
800	105	105	90	90	90	45	60	60	45	45	45
	800	150	175	150	105	60	90	90	60	60	60
		800	200	175	175	90	105	105	75	90	75
			800	200	200	105	135	120	90	105	90
				800	600	200	175	135	105	120	105
					800	600	200	150	120	135	120
						800	600	200	135	150	135
							800	600	400	200	150
								800	600	400	200
									800	600	400
										800	600
											800